The Adult Göttingen Minipig as a Model for Chronic Heart Failure After Myocardial Infarction: Focus on Cardiovascular Imaging and Regenerative Therapies

Karl H Schuleri,[1,2,]* Andrew J Boyle,[3] Marco Centola,[1,2] Luciano C Amado,[1] Robert Evers,[1] Jeffrey M Zimmet,[1] Kristine S Evers,[1] Katherine M Ostbye,[1] Diana G Scorpio,[4] Joshua M Hare,[5] and Albert C Lardo[1,2]

Porcine models have become increasingly popular in cardiovascular research. The standard farm pig rapidly increases in body weight and size, potentially confounding serial measurements of cardiac function and morphology. We developed an adult porcine model that does not show physiologic increases in heart mass during the study period and is suitable for long-term study. We compared adult minipigs with the commonly used adolescent Yorkshire swine. Myocardial infarction was induced in adult Göttingen minipigs and adolescent Yorkshire swine by occlusion of the left anterior descending coronary artery followed by reperfusion. At 8 wk after infarction, the left ventricular ejection fraction was 34.1 ± 2.3% in minipigs and 30.7 ± 2.0% in Yorkshire swine. The left ventricular end-diastolic mass in Yorkshire pigs assessed by magnetic resonance imaging increased 17 ± 5 g, from 42.6 ± 4.3 g at week 1 after infarction to 52.8 ± 6.6 g at week 8, whereas it remained unchanged in minipigs. Cardiac anatomy and physiology in adult minipigs were evaluated invasively by angiography and noninvasively by Multidetector Computed Tomography and by Magnetic Resonance Imaging at 1.5 T and 3 T prior to myocardial infarction and during follow-up. This porcine heart failure model is reproducible, mimics the pathophysiology in patients who have experienced myocardial infarction, and is suitable for imaging studies. New heart failure therapies and devices can be tested preclinically in this adult animal model of chronic heart failure.

Abbreviations: CEMRA, contrast-enhanced magnetic resonance angiography; CI, confidence interval; ECG, electrocardiogram; LAD, left anterior descending artery; LV, left ventricle; LVEF, left ventricular ejection fraction; MDCT, multidetector computed tomography; MI, myocardial infarction; MRI, magnetic resonance imaging

In the United States alone, 7.1 million people are survivors of myocardial infarction (MI) and 4.9 million people live with congestive heart failure.[4] New medical therapies, surgical procedures and devices for heart failure all rely heavily on preclinical testing in animal models. Porcine models of MI are used because of the similarities between porcine and human hearts.[29,38] However, the commonly employed farm pigs are utilized at a young age, grow rapidly and continue to gain in mass during use, thereby complicating long-term follow-up. The utilization of farm pigs at a young age, while their hearts are still growing does not accurately reflect the remodeling that occurs in adult patients after MI and can limit accurate assessment of chronic remodeling processes. This inaccuracy can confound evaluation of devices and pharmacologic therapies.

Noninvasive imaging techniques for determining anatomic and functional manifestations of congestive heart failure are ac-curate and reliable, and are used as surrogate markers of outcome and safety in phase I/II trials.[15,34] Cardiovascular imaging improves evaluation of the effects of new therapies and devices during preclinical assessment. Animal models of congestive heart failure should allow noninvasive imaging during a long-term follow-up period.

The Göttingen minipig was developed in the early 1960s at the Institute of Animal Breeding and Genetics (University of Göttingen, Germany) to reduce space requirements and housing costs for preclinical porcine studies.[9] They were created by crossbreeding the Minnesota minipig with Vietnamese potbelly and German Landrace pigs.[19] Göttingen minipigs are white miniature pigs with good fertility and stable genetics.

Göttingen minipigs have a characteristic growth curve that avoids the dramatic increase in weight in adulthood seen in farm pigs.[25,26] A newborn Göttingen minipig has a body mass of 350 to 450 g. Boars become sexually mature at 3 to 4 mo of age, weighing 6 to 8 kg, whereas sows become sexually mature at 4 to 5 mo and 7 to 9 kg. The gestational period is 112 to 114 d, and the average litter size is 5 to 6 animals. Closure of the growth plates is complete at 18 to 22 mo and 30 to 35 kg. Göttingen minipigs have a mature body weight of 35 to 45 kg,[10] and they achieve 40% of the maximal body weight at approximately 10 mo (310 d) with a body weight of 21 kg. In comparison intensively fed farm pigs

reach 88 kg at the same time point, with a mature weight of 220 kg, and restrictively fed farm pigs, like Yorkshire swine, typically weigh about 64 kg at 10 mo of age and 160 kg at maturity.[26] Characteristics of Yorkshire swine are reported in the literature.[11]

Adult Göttingen minipigs are large enough to allow testing of human equipment and devices. Until now cardiovascular parameters have only been reported in juvenile Göttingen minipigs.[9,13] Here, we demonstrate the unique value of Göttingen minipigs as a novel adult porcine heart failure model for cardiac research in the fields of regenerative medicine, electrophysiology, and noninvasive imaging.

Materials and Methods

Göttingen minipig and Yorkshire swine demographic data. All animal studies were approved by the Johns Hopkins University Institutional Animal Care and Use Committee and comply with the Guide for the Care and Use of Laboratory Animals.[21]

Forty-nine female Göttingen minipigs were purchased from Marshall BioResources (North Rose, NY). Animals from the same supplier were used in all experiments, and the growth curve after MI was generated from data acquired at Johns Hopkins University. Twenty-four Yorkshire swine purchased from Thomas D Morris (Reisterstown, MD) were used for comparison; growth curves after MI were generated at Johns Hopkins University. Body weight data were obtained to illustrate the normal growth of Göttingen minipigs and Yorkshire swine.

Myocardial infarction model. Myocardial infarction was created by temporary balloon occlusion of the LAD coronary artery for 120 to 150 min, followed by reperfusion. Anesthesia was induced in 49 adult female Göttingen minipigs by intramuscular injection of ketamine (35 mg/kg BW). Intravenous access was obtained with a 21- or 22-gauge needle in the ear vein, and initially anesthesia was achieved with intravenous pentobarbital at 20 to 60 mg/kg. Göttingen minipigs were intubated with an endotracheal tube of 5 to 6 mm internal diameter, and general anesthesia was maintained with 1% to 3% isoflurane supplemented with oxygen.

A midline neck incision was made, and the right carotid artery was cannulated with an 8-French sheath; 5000 IU heparin was administered intravenously. Left ventriculography was performed in a left anterior oblique projection, with injection of dye through either a 7-French pigtail catheter with side-holes or a size 4 Judkins right guide catheter. Next, a size 4 Judkins right guide catheter or 'hockey stick' guide was used to cannulate the right and left coronary arteries for selective coronary arteriography. A 0.014-in. angioplasty guide wire then was inserted into the LAD under fluoroscopic guidance, and a 2.5 × 12-mm Maverick balloon (Boston Scientific, Natick, MA) was inflated to 4 atmospheres just distal to the second diagonal branch of the LAD. Complete cessation of flow in the LAD was confirmed by angiography (Figure 1 A, B). The balloon was left inflated for 2 to 2.5 h; lidocaine was infused intravenously throughout this time.

After deflation of the balloon, restoration of flow in the LAD was confirmed by angiography; spasm of the coronary artery was treated with 100 µg intracoronary nitroglycerin. Repeat left ventriculography confirmed the presence of an anterior wall myocardial infarction (Figure 2 A through F). The catheters and sheath were removed, and the carotid artery ligated (Figure 3).

Coronary flow reserve. Before and after coronary occlusion, the coronary flow reserve was measured to assess the integrity of microvascular function in the LAD of 7 Göttingen minipigs and 8 Yorkshire swine. A Doppler wire was inserted into the LAD. With the guide catheter in the ostium of the left main coronary artery, 150 µg nitroglycerin was injected into the coronary to prevent spasm of the coronary artery around the wire. After insertion of the wire, the steady-state average peak velocity was recorded (Figure 2 H, I). Next, maximal hyperemia was achieved with 40 µg intracoronary adenosine, as previously validated.[22,23] The ratio of average peak blood flow velocity at maximal hyperemia to average peak blood flow velocity at baseline was recorded as coronary flow reserve.

Electrocardiogram (ECG). All 12-lead ECGs were recorded at 25 mm/s, 40 Hz, and 10 mm/mV in anesthetized and immobilized Göttingen minipigs in the supine position. Data were analyzed on a MAC VU resting ECG analysis system (Marquette Electronics, Milwaukee, WI).

Magnetic Resonance Imaging (MRI). Global left ventricular (LV) function of Göttingen minipigs at baseline was assessed by using either a 1.5-T magnet (CV/i, GE Medical Systems, Waukesha, WI) or a 3-T magnet (TIM Trio, Siemens Medical Solutions, Erlangen, Germany). For comparison of Göttingen minipigs and Yorkshire swine all MRI images were acquired by using a 1.5-T MR scanner (CV/i, GE Medical Systems) at 1 and 8 wk after MI induction. On the 1.5-T MR scanner, global LV function was assessed by using a steady-state free precession pulse sequence[37] as previously described.[2,3] Image parameters were: repetition time, 4.2 ms; echo time, 1.9 ms; flip angle, 45°; matrix, 256 × 160; slice thickness, 8 mm; no gap; 125 kHz; field of view, 28 cm; and number of signal averages, 1.

At 3 T, true fast imaging with steady-state precession was the pulse sequence of choice for functional imaging due to the high contrast-to-noise ratio between the blood pool and myocardium and relatively short breath-hold times. The cine images were acquired by using a repetition time of 25 ms, an echo time of 1.0 ms, a flip angle of 50°, a receiver bandwidth of 930 Hz/pixel, and spatial resolution of $1.0 \times 1.0 \times 8$ mm³. To minimize breath hold times and reduce overall heating of the tissue, integrated parallel imaging techniques were used at factors of up to ×2. An additional retrospectively gated cine pulse sequence was used in 4 of the 8 total cases on the 3-T scanner when the true fast imaging with steady-state precession sequence had poor image quality secondary to magnetic susceptibility imaging artifacts. This backup sequence was a 2D fast low-angle shot pulse sequence with a repetition time of 29 ms, echo time of 4 ms, and flip angle of 12°. Temporal resolution was measured at 29 ms and as in the true fast imaging with steady-state precession sequence, integrated parallel imaging techniques were used at factors of ×2, and spatial resolution was maintained.

All cine images were analyzed by using a custom research software package (Cine Tool, GE Medical Systems). Endo- and epicardial borders of the LV were defined in both the end-diastolic and end-systolic frames, and standard LV function parameters were calculated to evaluate resting LV function.

Delayed contrast enhancement. After intravenous bolus injection of Gd- diethylenetriaminepentaacetic acid (0.2 mmol/kg; Magnevist, Berlex, Wayne, NJ), delayed contrast-enhancement images were acquired 15 min after injection by using an ECG-gated breath-hold, interleaved, inversion recovery and fast gradient-echo pulse sequence in end-diastole. Imaging parameters were: repetition time, 7.3 ms; echo times, 3.3 ms and approximately
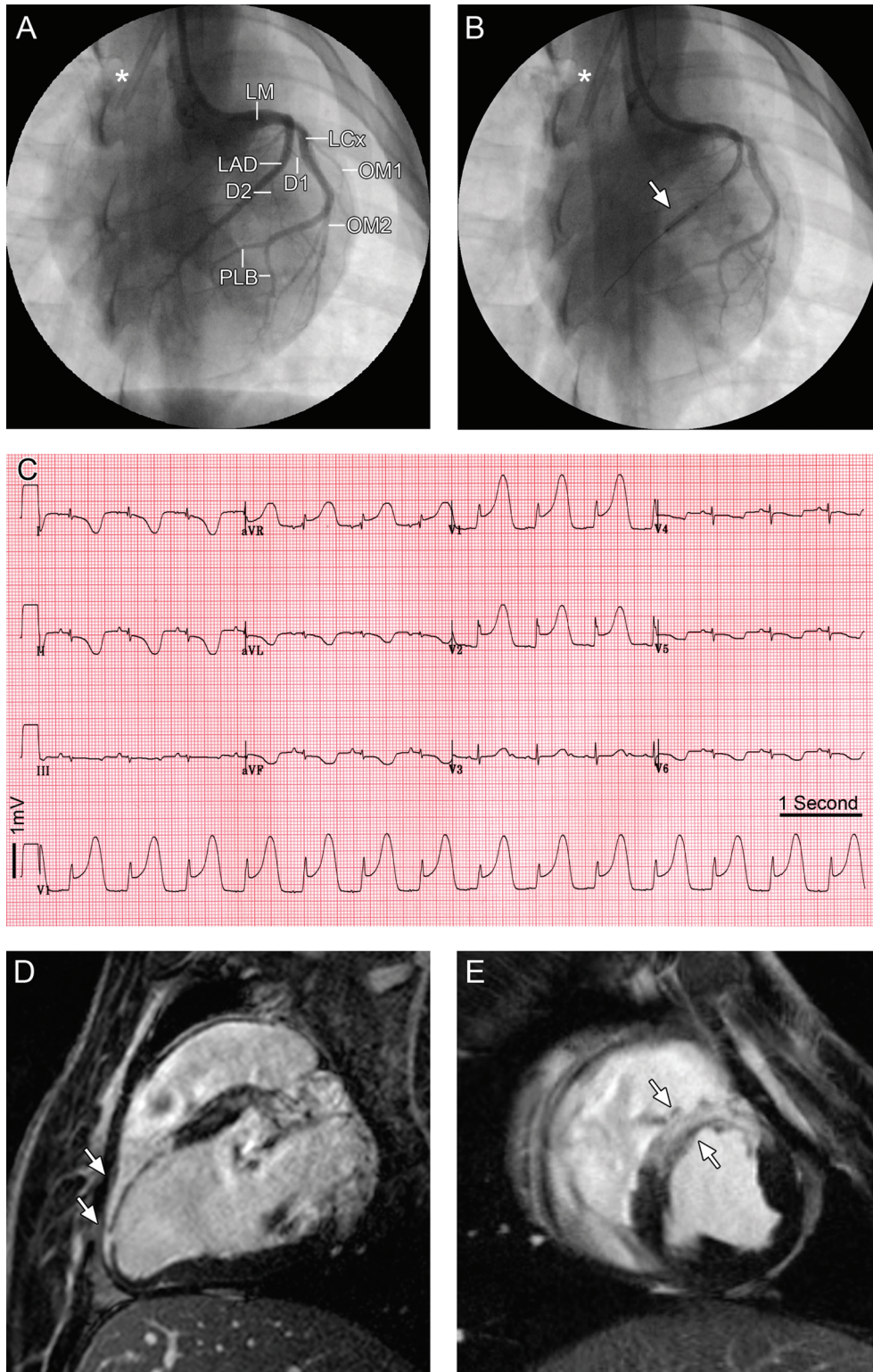
Figure 1. Acute myocardial infarct in a Göttingen minipig. (A) Normal left coronary tree with branching of the anterior descending artery (LAD) and the left circumflex coronary artery (LCx) from the left main coronary artery (LM) in anterior-posterior projection. The LAD gives rise to 2 major diagonal branches (D1 and D2) supplying the anterior wall of the left ventricle. The left circumflex coronary artery (LCx) gives rise to 2 large obtuse marginal branches (OM1 and OM2), continues and ends in 2 posterior lateral branches (PLB). (B) Balloon inflation for temporary occlusion of the LAD after D2 (arrow). The asterisk (*) indicates a permanent central line placed in the superior vena cava. (C) The 12-lead ECG acquired 5 min after balloon occlusion shows the anterior-lateral location of the infarct with ST-segment depression in leads I, II, aVL, and aVF, and 'tombstone' ST elevation in the precordial leads. (D, E) Examples of delayed enhancement MRI of the same animal acquired on a 3-T magnet 3 d after MI to verify the anteroseptal location and demonstrate the transmurality of the induced MI (white arrows) along the (D) long axis and (E) short axis.
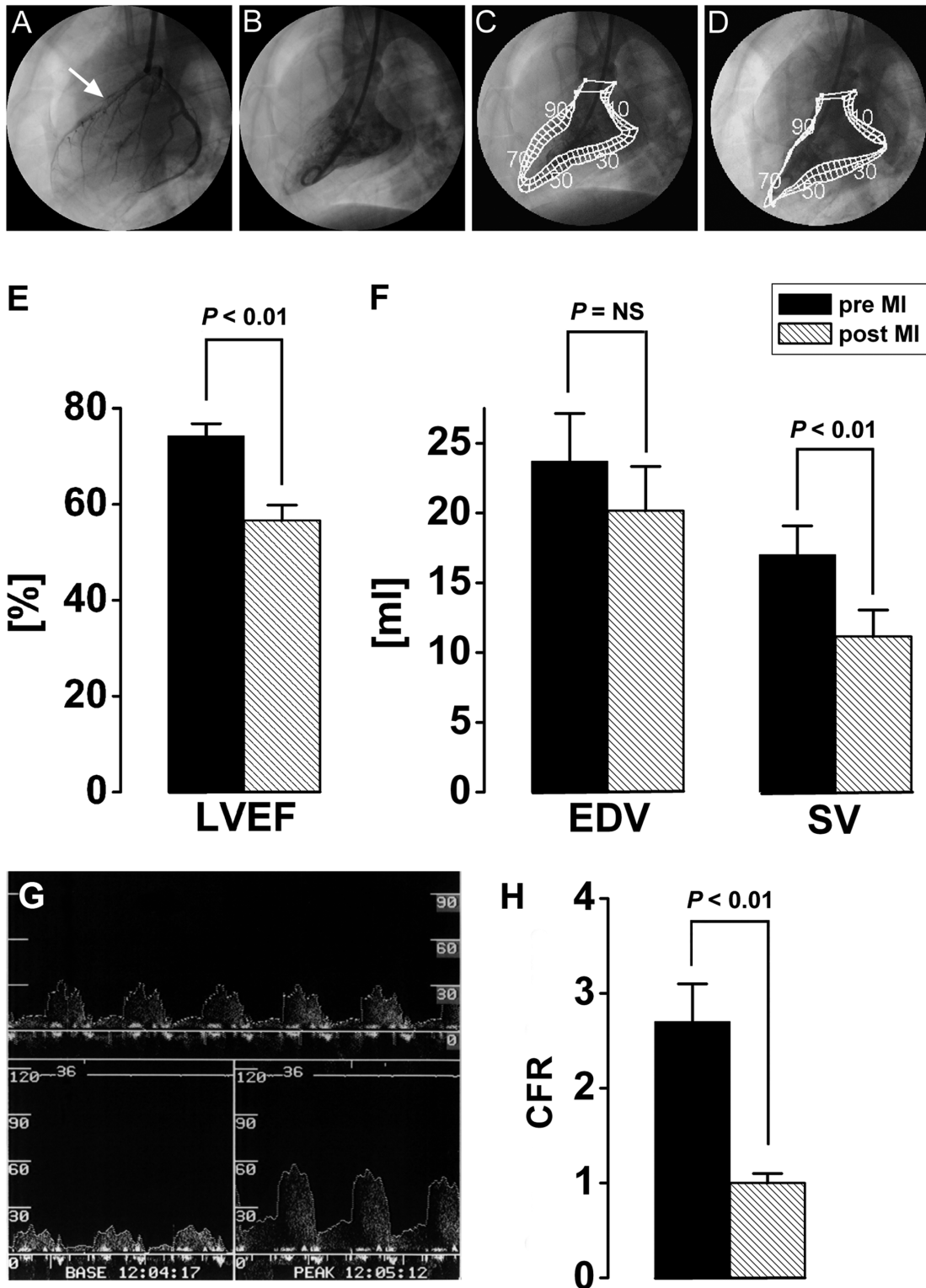
Figure 2. Left ventricular ejection fraction (LVEF) and left ventricular volumes before and after coronary occlusion. (A) Representative coronary angiogram of the anterior descending artery (LAD) and the left circumflex coronary artery (LCx) in lateral projection. The white arrow indicates the location of the LAD occlusion. (B) Ventriculogram of the left ventricle in the same projection as the coronary angiogram. Normal wall motion of the left ventricle assessed by the center line method (C) before (pre) and (D) 2.5 h after (post) coronary occlusion. The center line method demonstrates loss of left ventricular contractility in the anterior wall chords (E) LVEF dropped from 74.3% ± 2.5% before MI to 56.9% ± 3.2% afterward ($P < 0.01$). (F) Although the EDV remained unchanged in the Göttingen minipigs immediately after MI, (G) the stroke volume (SV) showed significant ($P < 0.01$) reduction. (H) Coronary flow reserve in the LAD before MI. The top panel shows real-time Doppler flow in the artery, the bottom left panel demonstrates the baseline flow, and the bottom right panel shows peak Doppler flow at maximal hyperemia after administration of adenosine. (I) Measurement of the coronary flow reserve before and after LAD occlusion demonstrates the microvascular impairment after acute MI.
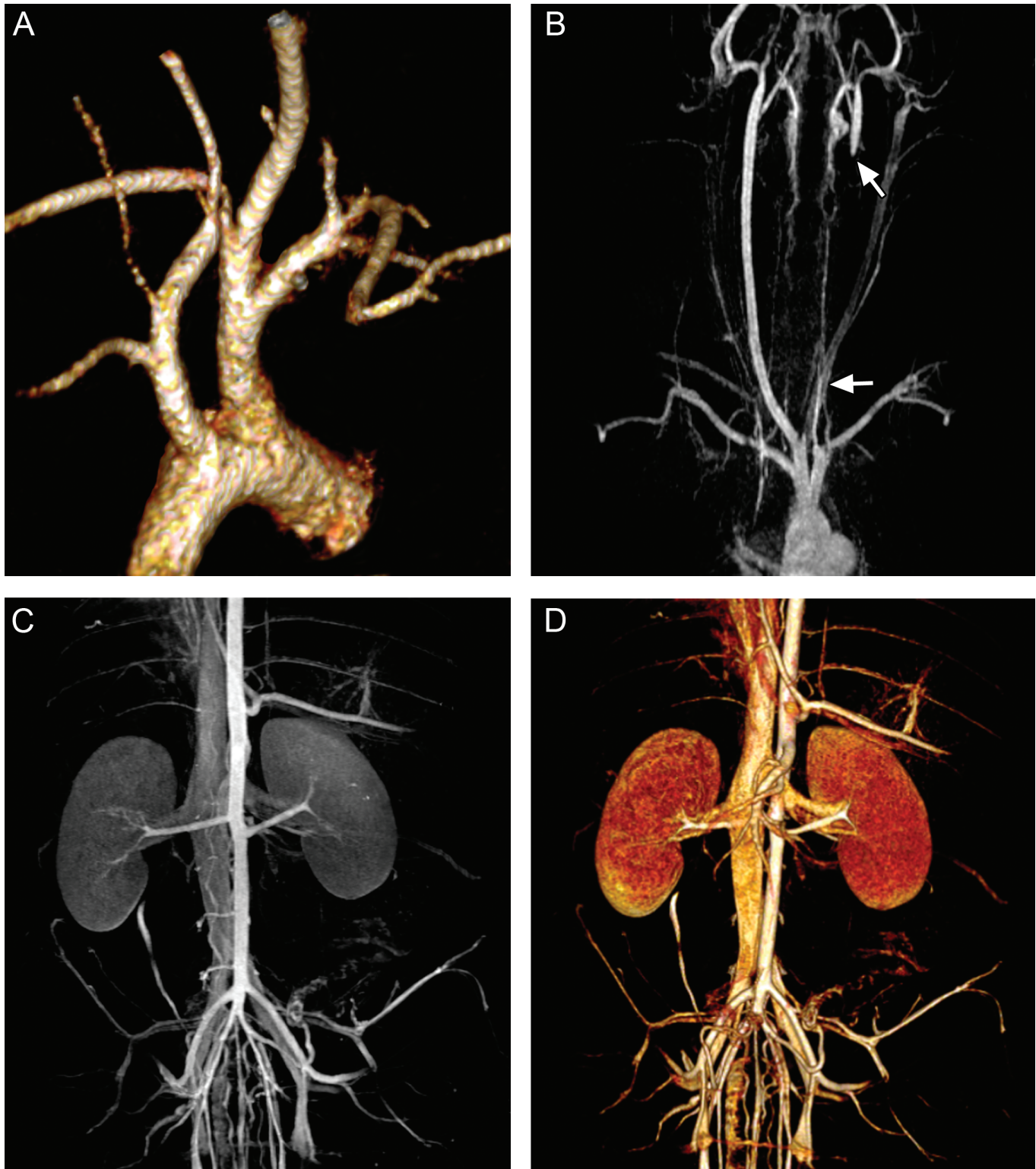
Figure 3. Three-dimensional Gd-MR angiography at 3 T. (A) Volume-rendered images of the aortic arch. (B) Maximum-intensity projection (MIP) of the carotid arteries shows the vessels extending from the aortic arch. The white arrows indicate the location where the carotid arteries were ligated after the MI procedure. (C) MIP and (D) volume-rendered image of the renal vessels demonstrate the arterial and venous supply of the kidney.

200 ms; flip angle, 25°; matrix, 256 × 196 to 160; slice thickness, 8 mm; no gap; 31.2 kHz; field of view, 28 cm, and number of signal averages, 2. Inversion recovery times were adjusted as needed to suppress the signal of the viable myocardium and obtain an even, dark appearance of the viable myocardium, thereby increasing the contrast-to-noise ratio for better visualization of the infarct scar.[36] All delayed contrast-enhancement images were analyzed by using Cine Tool. Endo- and epicardial borders of the LV were defined manually, and infarct areas were calculated based on the full width at half-maximum criterion.[1]

Contrast-enhanced MR angiography. Vascular imaging of the aortic arch and great vessels as well the abdominal aorta and iliac arteries was performed by using a noninvasive contrast-enhanced MR angiography technique. Imaging was completed on a 3.0-T magnet (TIM Trio, Siemens Medical Solutions). Gadopentetate dimeglumine was injected intravenously at a dose of 0.1 mmol/kg and rate of 2 ml/s with a 30-ml bolus saline flush. To ensure arterial phase angiographic capturing of data, imaging was completed by using CARE Bolus computed tomography (fluoroscopic triggering; Siemens Medical Solutions) in conjunction with immediate central k-space filling at the onset of 3D-imaging. Three-dimensional gadolinium-enhanced magnetic resonance angiograms were acquired with an ultrashort 3D fast low-angle shot sequence: repetition time, 3.0 ms; echo time, 1.0 ms; flip angle, 13°; receiver bandwidth, 500 Hz per pixel; and spatial resolution of 1.2 × 1.2 × 2 mm³. To minimize breath-hold times and reduce overall tissue heating parallel imaging techniques were employed.

Multidetector computed tomography (MDCT). Göttingen minipigs were anesthetized as described and immobilized in the supine position with vector ECG leads in place. General anesthesia was maintained with inhaled isoflurane throughout the study period. Each animal was scanned by using a 0.5 mm × 64-detector scanner (Aquilion TM64, Toshiba Medical Systems, Otawara, Japan). Animals received intravenous metoprolol (2 to 5 mg) or amiodarone (50 to150 mg) or both to achieve a heart rate 60 to 80 beats per minute. After scout acquisition and slice prescription, a 150-ml bolus of iodixanol (Visipaque, 320 mg iodine/ml, Amersham Health, Buckinghamshire, UK) was injected intravenously. During MDCT acquisition respiration was suspended for 30 to 60 s, depending on the heart rate, and imaging was performed by using a retrospectively gated MDCT protocol with the following parameters: gantry rotation time, 400 ms; detector collimation, 0.5 mm × 64 (isotropic voxels = 0.5 × 0.5 × 0.5 mm³; 13 line pairs/cm); helical pitch, variable depending on heart rate (range, 6.4 to 8.8); tube voltage, 120 kV; and tube current, 400 mA).

Statistics. Linear models with third-order polynomial structure of fit were applied to demonstrate gain in body weight in Yorkshire swine and in infracted and not infracted Göttingen minipigs, as described in detail elsewhere.[26] All data are presented as mean ± SEM unless otherwise stated. Normal distribution was evaluated for body weight, age, left ventricular MRI and angiography data, and ECG and hematology values were examined with the Kolmogorov–Smirnov test. P values were calculated with Dallal and Wilkinson approximation to the Lilliefors method. All data sets show a Gaussian distribution with P values greater than 0.1, except LVED mass for MRI ($P = 0.04$). MRI and LV angiography were compared by using the Pearson correlation coefficient. Agreement between the 2 methods was assessed by Bland–Altman analysis and expressed as mean ± SD difference at the 95% confidence interval (CI).

MRI values at weeks 1 and 8 and LV angiogram parameters before and after MI were compared between groups by using the Student t test. Dichotomous variables including mortality and presence of arrhythmias are analyzed by using Pearson χ^2 and Fishers exact tests. Inter- and intragroup comparison of Göttingen minipigs and Yorkshire swine were evaluated with paired or unpaired Student t tests when appropriate. P values less than 0.05 are considered significant. All analyses were performed with commercially available software (GraphPad Software, La Jolla, CA, and MedCalc Software, Mariakerke, Belgium).

Results

Göttingen minipig demographic data. Yorkshire swine continued to accumulate body weight rapidly after adolescence. In contrast, the growth of Göttingen minipigs slowed once adulthood is reached (Figure 4).

At the time of infarction, the 49 Göttingen minipigs studied had a mean weight of 29.6 ± 0.5 kg and were 15.1 ± 0.7 mo old. At this age, Göttingen minipigs are considered adult animals. We used the Göttingen minipigs at the same body weight as the Yorkshire swine (age, 4 to 6 mo) for the MI procedure. The Göttingen minipigs showed a modest 10% increase in body weight with or without MI over 2 mo follow-up (Table 1), whereas the Yorkshire swine gained 29% in body weight over the same time period (Figure 5 A through C).

Cardiac analysis. Like other swine species, Göttingen minipigs have a coronary artery anatomy similar to that of humans. The left coronary artery divided into the LAD and left circumflex branches (Figures 1, 6). The right coronary artery was dominant in 90% of cases, with the distal left circumflex branch supplying the posterior descending artery in the other 10%. In animals with right-dominant circulation, the right coronary artery supplied a small left ventricular branch in addition to the posterior descending artery in 55% of animals. However, Göttingen minipigs have a smaller LAD than do other pig species.

We used MRI to evaluate normal left ventricular values in 22 Göttingen minipigs at 14.9 ± 1.1 mo before the MI procedure (baseline assessment). Overall, the left ventricular ejection fraction (LVEF) ranged from 45.7% to 61.1%, with a mean of 51.6 ± 0.8%. The complete set of normal left ventricular volumes is shown in Table 2. In 20 animals, the LVEF was measured by angiographic ventriculography and ranged from 51.4% to 90.1%, with a mean of 72.76% ± 2.26%. The normal values for LVSV, LV end-diastolic volume, and LV end-systolic volume for adult Göttingen minipigs by angiography are shown in Table 3. MRI measurement of the LVEF showed good correlation to angiographic ventriculography (r = 0.65; $P < 0.0001$). Bland–Altman analysis of LV angiograms and MRI revealed a mean difference of 25.8% in LVEF. Compared with MRI, angiographic ventriculography overestimated LVEF.

ECG. Normal values for 12-lead ECG recordings from 15 adult Göttingen minipigs are presented in Table 4. Previous reports in the literature have not described any conduction abnormalities in Göttingen minipigs. We detected first-degree atrioventricular blocks in 3 of the 15 (20%) baseline ECGs from adult female Göttingen minipigs. Figure 1 and 7 show characteristic ECG changes during MI and after reperfusion.

Myocardial infarction model. Myocardial infarction was accomplished in all pigs by using standard guide catheters, 0.014-in. wires, and standard angioplasty balloons. Although the carotid arteries were situated more deeply in the necks of the Göttin-
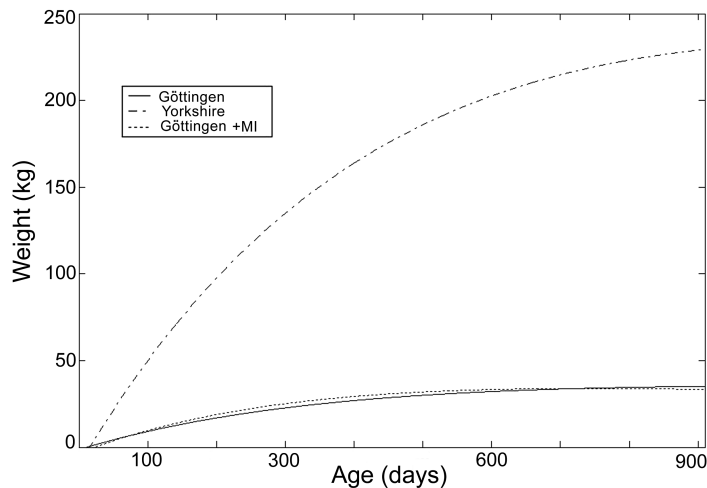
Figure 4. Growth curves of Yorkshire swines and Göttingen minipigs with and without myocardial infarction at our institution as predicted by the third-order polynomial function.

Table 1. Body weight in Göttingen minipigs with and without myocardial infarction (MI)

	With MI (n = 12)		Without MI (n = 8)		P
Age at baseline (d)	395.3	± 15.1	362.0	± 13.8	0.12
Age at baseline (mo)	13.2	± 0.5	12.1	± 0.5	
Follow-up (d)	62.7	± 1.2	68.5	± 13.0	0.67
Weight at baseline (kg)	30.1	± 1.1	28.3	± 1.4	0.31
Weight at week 8 (kg)	33.1	± 1.1	31.0	± 1.3	0.27
Weight change from baseline (%)	10.1	± 1.8	10.2	± 3.0	0.99

gen minipigs than in the Yorkshire swine, access to the carotid artery was readily achieved with a little practice. The aortic arch is smaller and more angulated in Göttingen minipigs, and in our experience, access to the coronary arteries through the carotid artery was easier than through the femoral arteries. No neurologic symptoms were noted when both carotid arteries were ligated, allowing arterial access to be achieved twice in each animal. The coronary arteries of Göttingen minipigs were more prone to spasm than those of Yorkshire swine, but spasms were easily preventable with intracoronary nitroglycerin prior to insertion of the guide wire.

Mortality from anterior MI did not differ significantly between the animals and was 18% in Göttingen minipigs and 17% in Yorkshire swine. The Göttingen minipigs appeared to be more resistant to arrhythmia, with 29% (14 of 49) developing ventricular fibrillation during or immediately after balloon occlusion of the LAD. In contrast, 63% (15 of 24) of the Yorkshire swine showed ventricular fibrillation during or immediately after balloon occlusion (*P* = 0.01). However, Yorkshire swine were more likely to survive the arrhythmias with cardioversion than were Göttingen minipigs, resulting in similar overall mortality rates.

Occlusion of the LAD after the second diagonal branch reliably resulted in MI in Göttingen minipigs (Figures 1, 7). Occlusion after the first diagonal branch in Yorkshire swine and the Göttingen resulted in the same size of infarct (Figure 5 D, E), but Göttingen minipigs did not survive this type of occlusion. Immediately after

MI, microvasular function in the infarcted territory was impaired, as demonstrated by reduction in coronary flow reserve as measured by intracoronary Doppler flow (Figure 2 H, I). MI results in immediate reduction in LVEF and systolic volume after reperfusion (Figure 2 E, F). Ongoing remodeling of the left ventricle was evident by continued reduction in LVEF over the following 8 wk (Figure 5 F). This mimics the LV remodeling seen in adult humans after MI.[32]

Noninvasive cardiovascular imaging. Representative results for cardiovascular imaging are presented for MDCT and MRI using clinical applicable protocols. High-quality coronary angiography is feasible in the Göttingen minipig (Figure 6). Cardiac MRI at 1.5 and 3 T yielded highly reproducible results (Figure1 and 5) and can be applied for the evaluation of disease progression or therapy. Standard MR angiography protocols can be used in the Göttingen minipig to assess the anatomy of the arterial and venous vessel system (Figure 3).

Göttingen minipigs showed an MI volume similar to that of Yorkshire swine at week 1 after MI (6.3 ± 0.7 ml versus 6.8 ± 1.0 ml, respectively), although the LAD was commonly occluded after the first diagonal branch in Yorkshire swine but after the second in Göttingen minipigs. Despite infarct expansion over 8 wk, the MI volumes remained unchanged (at week 8: Göttingen minipigs, 7.1 ± 1.0 ml; Yorkshire swine, 7.4 ± 1.2 ml; Figure 5 D). The MI size in relation to the LV mass tended to be larger in Göttingen minipigs at week 8 (21.1% ± 2.9% versus 4.3% ± 2.5% in Yorkshire swine; *P* < 0.05; Figure 5 E). However, both animal models showed similar marked decreases (*P* < 0.05) in LVEF during follow-up after MI (week 8: Göttingen minipigs, 34.1% ± 2.3%; Yorkshire swine, 30.7% ± 2.0%). The LVEF dropped earlier and tended to be lower in Yorkshire swine than Göttingen minipigs (Figure 5 F).

Discussion

Animal models of human disease should represent the human clinical disease as accurately as possible. In chronic postinfarction heart failure models, MI sizes have to be highly reproducible, with acute reduction in regional and global LV function. With an increasing demand for large animal models to evaluate heart
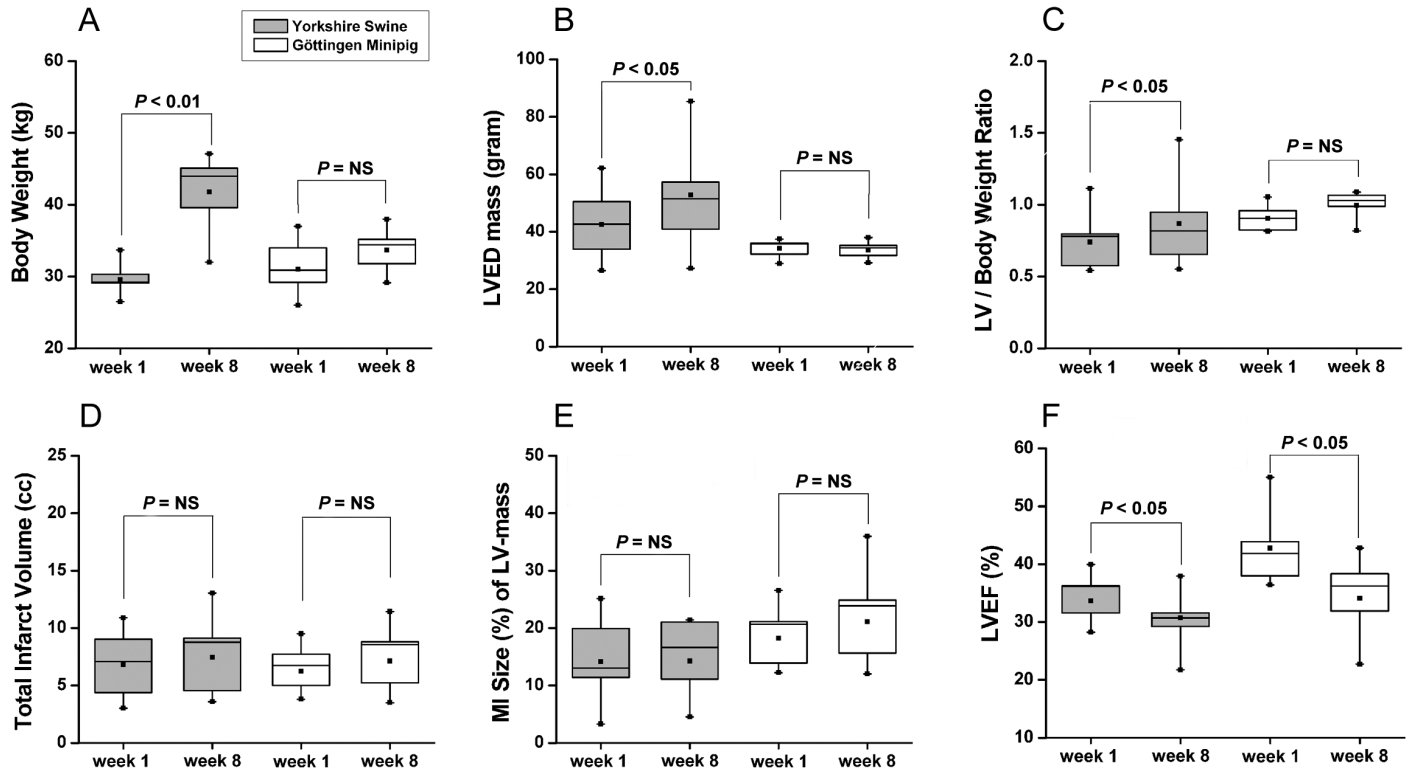
Figure 5. Comparison of body weight and LV parameters 1 and 8 wk after MI in Yorkshire swine (n = 8) and Göttingen minipigs (n = 8). (A) Whereas Yorkshire swine increase in body weight, Göttingen minipigs do not. (B) LV end-diastolic mass increases in Yorkshire swine. (C) The increase in LV end-diastolic mass in Yorkshire swine remains significant even when the LV mass is corrected for body weight. (D) Similar MI volumes in both animal models. (E) MI size relative to LV mass tends to be larger in Göttingen minipigs. (F) Both models show a significant drop in LVEF after MI.

failure therapies, especially for the rapidly developing fields of regenerative medicine, electrophysiology, and noninvasive imaging,[40] we aimed to establish the Göttingen minipig as an adult animal model for chronic heart failure after MI for long-term follow-up.

We characterized the normal cardiac function and physiology in the adult Göttingen minipigs. Normal LVEF MRI values of Göttingen minipigs are lower than human reference values.[31] In the catheterization laboratory we used only a single lateral projection to evaluate LV function in the minipigs with ventriculography, and the contrast material was injected manually. However, our results compare favorably with human data using the lateral projection[40] and biplanar anterior-posterior and lateral projections.[18,24] As reported for human values,[27] the angiographic LV data of the Göttingen minipig showed overestimation of LV function and volumes, compared with MRI data.

Animal models[33] and human studies[39] have demonstrated that moderate-sized infarcts result in the most LV remodeling, and these subjects have the best response to therapies. Our model reliably resulted in transmural anterior MI that led to LV remodeling with an LVEF of 34.1% ± 2.3% after 8 wk. This outcome reflects chronic heart failure with moderate LV impairment and is therefore an excellent model for chronic heart failure to mimic human disease. In addition, this LVEF range is the level at which implantable cardioverter–defibrillator device therapy is considered. The Göttingen minipig model, therefore, also may lend itself to studies of device therapy for heart failure. Overall, population studies of heart failure have shown that LVEF is a powerful predictor for

outcome[17] and is therefore a good surrogate marker to evaluate new therapies. As demonstrated, reliable LVEF parameters can be obtained invasively by conventional angiography or noninvasively by MRI of Göttingen minipigs.

Our ECG findings are in agreement with previous evaluations in larger cohorts of conscious but younger Göttingen minipigs.[9,13] However, for the first time, we report ECG values derived from 12-lead registrations for adult Göttingen minipigs older than 12 mo. The prolonged QT interval in Göttingen minipigs first was described in the 1970s and was viewed as a favorable ratio of systolic and diastolic phase.[9] Interestingly, despite a prolonged QT interval at baseline, these animals are comparatively resistant to ventricular arrhythmias induced by myocardial ischemia. Yet, if ventricular fibrillation does develop, Göttingen minipigs are more difficult to electrically cardiovert to sinus rhythm than are Yorkshire swine. Göttingen minipigs show abundant premature ventricular complexes during the first 30 min to 60 min after balloon occlusion, comparable to observations in human patients before the era of aggressive reperfusion therapies.[12] We did not use intensive antiarrhythmic regimens including amiodarone or β-blockers to suppress premature ventricular contractions and ventricular tachycardia during the infarct procedure in either pig species. Although these pharmacologic approaches can reduce infarct mortality, they also reduce infarct size significantly,[20] which is not warranted in this chronic heart failure model.

The Göttingen minipig is especially suitable for long-term studies because of its inherent small size and ease of handling, even at full maturity, which is reached at 2 y of age compared with 3 y for
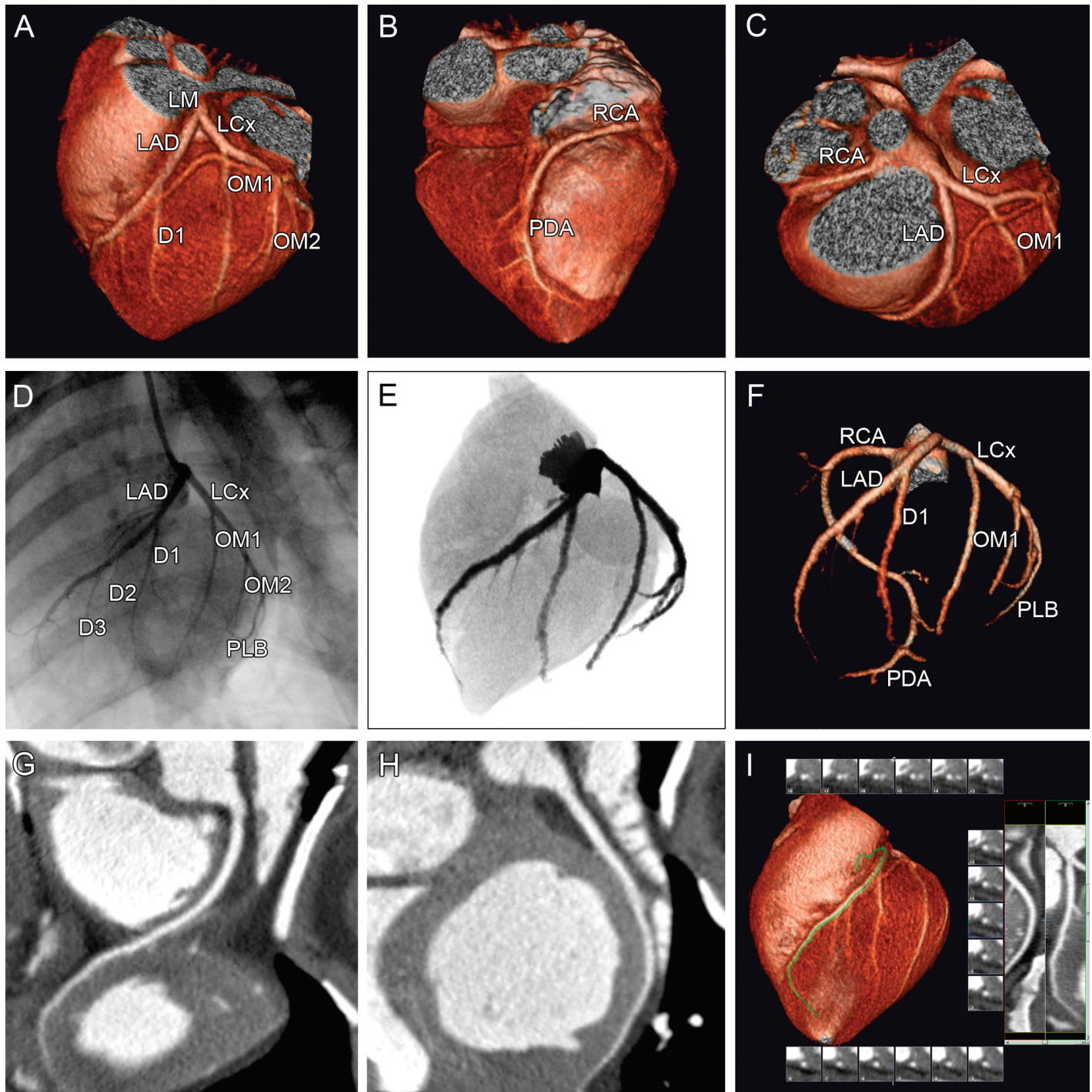
Figure 6. MDCT images of a normal Göttingen minipig heart and coronary arteries. All images were acquired from the same minipig heart. The upper panel shows the 3D reconstructions. (A) This anteriocranial projection shows the coronary blood supply for the anterior part of the left ventricle. The LAD and the left circumflex coronary artery (LCx) originate from a short left main coronary artery (LM). The LAD first gives off a large diagonal branch (D1). The LCx gives rise to 2 large obtuse marginal branches (OM1 and OM2). (B) In this posterior projection, the right coronary circulation is visualized. The right coronary artery (RCA) descends into the posterior interventricular groove to provide the posterior descending artery (PDA). (C) From the cranial projection the branching of the RCA and the LM dividing into the LAD and LCx can be appreciated. The middle panels show the left coronary vessel system in an anteriolateral projection visualized by (D) conventional coronary angiography and (E) coronarycomputed tomography angiograms eformatted to a conventional angiographic view. (F) Maximum-intensity projection of the coronary tree displays all of the main coronary arteries and the major branches. The bottom panel shows the (G) RCA and (H, I) LAD in a multiplanar reformat, which is used clinically to determine the severity and extent of atherosclerotic plaques.

Table 2. Normal left ventricular values in adult Göttingen minipigs by MRI

	Mean	SD	SE	Lower limit of 95% CI	Upper limit of 95% CI
Ejection fraction (%)	51.6	3.6	0.8	50.0	53.2
Systolic volume (ml)	19.4	3.8	0.8	17.7	21.0
End-diastolic volume (ml)	37.9	8.9	1.9	34.0	41.9
End-systolic volume (ml)	18.6	5.3	1.1	16.2	20.9
End-diastolic mass (g)	28.6	7.2	1.5	25.4	31.8
End-systolic mass (g)	39.1	6.6	1.4	36.2	42.1

Table 3. Normal left ventricular values in adult Göttingen minipigs by angiography

	Mean	SD	SE	Lower limit of 95% CI	Upper limit of 95% CI
Ejection fraction (%)	72.7	10.1	2.3	68.0	77.4
Systolic volume (ml)	18.0	9.9	2.2	13.4	22.6
End-diastolic volume (ml)	25.3	15.0	3.4	18.2	32.3
End-systolic volume (ml)	7.3	6.2	1.4	4.4	10.2

Table 4. Normal electrocardiogram values for adult Göttingen minipigs

	Mean	SD	SE	Lower 95% CI of mean	Upper 95% CI of mean
Ventricular rate (beats per min)	104	15	4	95	112
PR interval (ms)	122	16	5	112	132
QRS duration (ms)	59	5	1	56	62
QT (ms)	360	45	12	335	385
QTc (ms)	467	39	10	445	489

domestic pigs.[10] The adult body weight of the Göttingen minipig at an age of 2 years is 35 to 40 kg.[10] At that time, the body weight of other minipig species like the Yucatan minipig, which is widely used in cardiovascular research, and the Hanford minipig is already 70 to 90 kg.[11] We demonstrate that in this model, a standard farm pig, like the Yorkshire swine, increases 29% ± 3% in body weight during a 2-mo follow-up after MI (Figure 5 A). Our findings are consistent with those of other investigators,[19,28] who report even more dramatic increases of 45% ±6% and 60% ± 6% in body weight over 2 mo after MI in farm pigs. One of these studies[19] presents 12-wk follow-up data after MI in control animals, reporting an increase in body weight from 29 ± 1.9 kg to 101.6 ± 9.6 kg and a change in heart weight evaluated by MRI from 63.5 ± 8.2 g to 175.9 ± 23.3 g. In the present study, not only body weight but also heart weight continued to increase in juvenile Yorkshire swine (Figure 5 B, C), and these changes can confound the evaluation of new therapeutic approaches, particularly for regenerative therapies. The juvenile Yorkshire swine model does not reflect the situation seen in adult cardiac patients. We consider that follow-up and high-quality imaging will be feasible for 6 to 8 mo (or even longer) after MI in Göttingen minipigs. Importantly, in contrast to the commonly used Yorkshire swine, Göttingen minipigs can be used as adult animals. Previous studies[5,6] investigated the effect

of aging on heart muscle physiology and pathophysiology and demonstrated quite different therapeutic success with regenerative therapy depending on biological age.[30]

The Göttingen minipig is amendable to all currently used imaging techniques that have been used to demonstrate safety and efficacy in clinical stem cell trials. In the largest randomized controlled trial to date, invasive LV angiography[7,35] and coronary flow reserve values[14] were used to demonstrate benefit from stem cell delivery, whereas MRI was the most commonly used noninvasive method to assess LV function and volumes.[8] The Göttingen minipig allows invasive and noninvasive evaluation of the functional effects of regenerative therapy. Therefore, experimental results in this animal model can easily be used to demonstrate the safety and efficacy of treatments and devices and to facilitate the translation of novel therapies into clinical applications.

In summary, we have developed and characterized an adult porcine model of chronic heart failure after MI that is amendable to current invasive and noninvasive imaging techniques and that is especially valuable for evaluating electrophysiologic devices and regenerative therapies. With an increasing interest in translational research to move scientific results more rapidly into the clinical arena without exposing patients to unnecessary risks, the Göttingen minipig model of chronic heart failure is a valuable addition to existing animal models of acute LV failure. Therapies and devices for chronic heart failure can be tested now in a valid preclinical adult animal model with reduced LVEF and chronic remodeled infarct scars. Long-term follow-up with evaluation by noninvasive imaging techniques is feasible and shows reproducible results of high quality.

References

1. **Amado LC, Gerber BL, Gupta SN, Rettmann DW, Szarf G, Schock R, Nasir K, Kraitchman DL, Lima JA.** 2004. Accurate and objective infarct sizing by contrast-enhanced magnetic resonance imaging in a canine myocardial infarction model. J Am Coll Cardiol **44:**2383–2389.
2. **Amado LC, Saliaris AP, Schuleri KH, St JM, Xie JS, Cattaneo S, Durand DJ, Fitton T, Kuang JQ, Stewart G, Lehrke S, Baumgartner WW, Martin BJ, Heldman AW, Hare JM.** 2005. Cardiac repair with intramyocardial injection of allogeneic mesenchymal stem cells after myocardial infarction. Proc Natl Acad Sci USA **102:**11474–11479.
3. **Amado LC, Schuleri KH, Saliaris AP, Boyle AJ, Helm R, Oskouei B, Centola M, Eneboe V, Young R, Lima JA, Lardo AC, Heldman AW, Hare JM.** 2006. Multimodality noninvasive imaging demonstrates in vivo cardiac regeneration after mesenchymal stem cell therapy. J Am Coll Cardiol **48:**2116–2124.
4. **American Heart Association** [Internet]. Heart and stroke statistics–2008 update. [cited 10 June 2008]. Available at http://circ.ahajournals.org/cgi/reprint/117/4/e25
5. **Anversa P, Ricci R, Olivetti G.** 1986. Quantitative structural analysis of the myocardium during physiologic growth and induced cardiac hypertrophy: a review. J Am Coll Cardiol **7:**1140–1149.
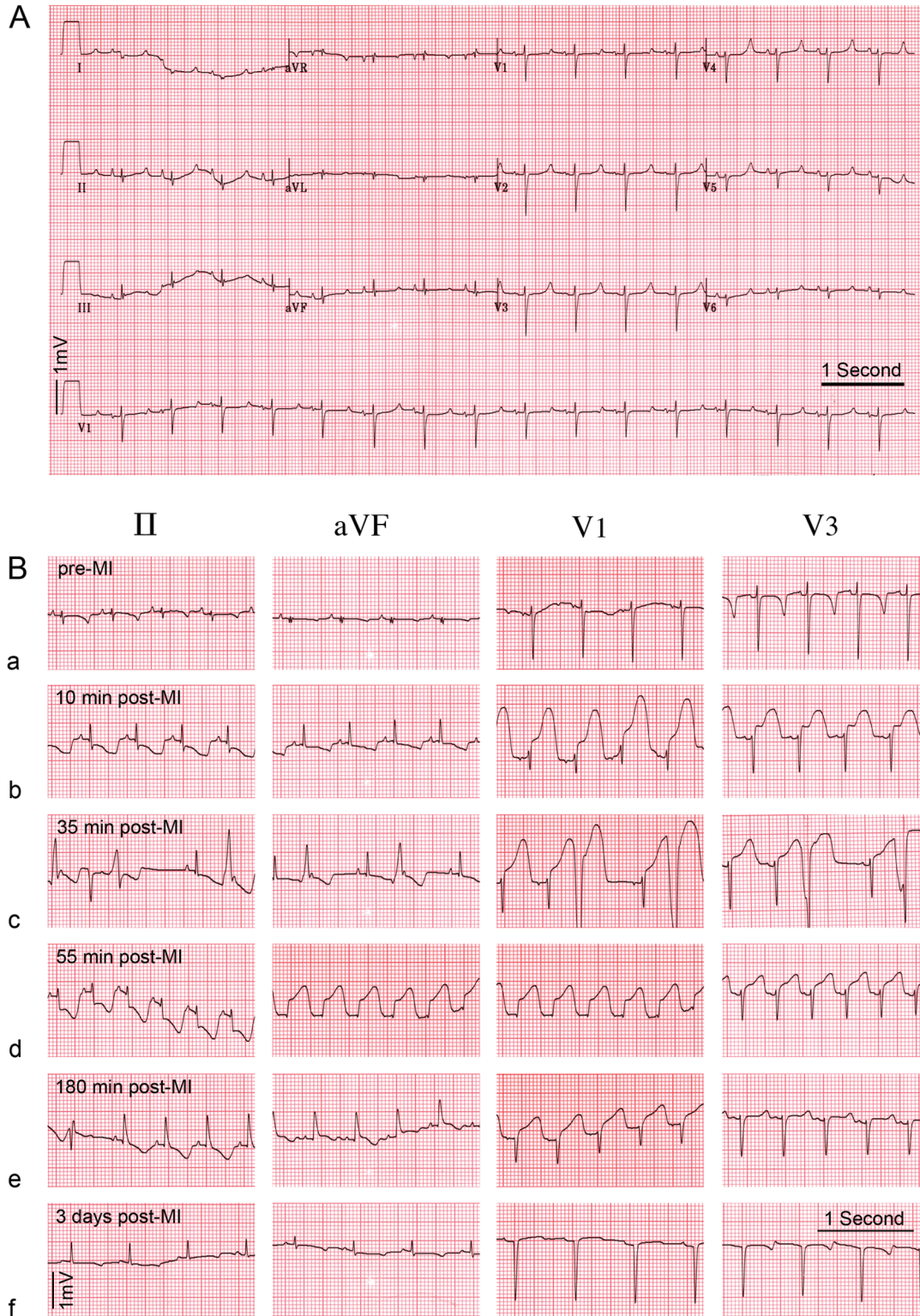
Figure 7. Example of twelve-lead ECGs in Göttingen minipigs (A) Example of a normal ECG in an anesthetized Göttingen minipig (25 mm/s). (B) ECG time course in a Göttingen minipig during the MI procedure. (a) Baseline ECG prior to MI induction. (b) At 10 min after balloon occlusion, sinus tachycardia (123 beats per minute) with a short PR interval (100 ms) is present, with marked ST depression in II and aVF and 'tombstone' ST elevation in V1 and V3 (c) At 35 min into the MI period, frequent (>5 per minute) and consecutive premature ventricular complexes occurred. (d) At 55 min after balloon occlusion, the animal developed ventricular fibrillation. After cardioversion, the animal developed ectopic atrial tachycardia (162 beats per minute), which reverted to sinus tachycardia. (e) At 2.5 h after balloon occlusion, the infarct territory was reperfused. The ECG shows sign of transmural infarction after removal of the balloon catheter. (f) ST depression, which is most prominent in the aVF lead, is present 3 d after MI.

6. **Anversa P, Rota M, Urbanek K, Hosoda T, Sonnenblick EH, Leri A, Kajstura J, Bolli R.** 2005. Myocardial aging–a stem cell problem. Basic Res Cardiol **100:**482–493.

7. **Assmus B, Honold J, Schachinger V, Britten MB, Fischer-Rasokat U, Lehmann R, Teupe C, Pistorius K, Martin H, Abolmaali ND, Tonn T, Dimmeler S, Zeiher AM.** 2006. Transcoronary transplantation of progenitor cells after myocardial infarction. N Engl J Med **355:**1222–1232.

8. **Beeres SL, Bengel FM, Bartunek J, Atsma DE, Hill JM, Vanderheyden M, Penicka M, Schalij MJ, Wijns W, Bax JJ.** 2007. Role of imaging in cardiac stem cell therapy. J Am Coll Cardiol **49:**1137–1148.

9. **Beglinger R, Becker M, Eggenberger E, Lombard C.** 1975. [The Goettingen miniature swine as an experimental animal. 1. Review of literature, breeding and handling, and cardiovascular parameters] Res Exp Med (Berl) **165:**251–263.

10. **Bollen P, Ellegaard L.** 1997. The Göttingen minipig in pharmacology and toxicology. Pharmacol Toxicol **80 Suppl 2:**3–4.

11. **Bollen PJA, Hansen AK. Ellegaard HL.** 1999 The laboratory swine. Boca Raton (FL): CRC Press.

12. **Cannom DS, Prystowsky EN.** 1999. Management of ventricular arrhythmias: detection, drugs, and devices. J Am Med Assoc **281:**172–179.

13. **Eckenfels A, Schuler S.** 1988. [The normal electrocardiogram of miniature swine] Arzneimittelforschung **38:**253–259.

14. **Erbs S, Linke A, Schachinger V, Assmus B, Thiele H, Diederich KW, Hoffmann C, Dimmeler S, Tonn T, Hambrecht R, Zeiher AM, Schuler G.** 2007. Restoration of microvascular function in the infarct-related artery by intracoronary transplantation of bone marrow progenitor cells in patients with acute myocardial infarction: the doppler substudy of the reinfusion of enriched progenitor cells and infarct remodeling in acute myocardial infarction (REPAIR-AMI) trial. Circulation **116:**366–374.

15. **Fernandes VR, Cheng S, Lima JA.** 2006. Atherosclerosis imaging and heart failure. Heart Fail Rev **11:**279–288.

16. **Gradman A, Deedwania P, Cody R, Massie B, Packer M, Pitt B, Goldstein S.** 1989. Predictors of total mortality and sudden death in mild to moderate heart failure. Captopril–Digoxin study group. J Am Coll Cardiol **14:**564–570.

17. **Graham TP Jr, Jarmakani JM, Canent RV Jr, Morrow MN.** 1971. Left heart volume estimation in infancy and childhood. Reevaluation of methodology and normal values. Circulation **43:**895–904.

18. **Haring F, Steinbach J, Scheven B.** 1963. [Züchtung eines Miniaturschweines als Versuchs und Laboratoriumstier]. Zentralbl Bakteriol Parasitenkd Infektionskr Hyg **189:**521–537.

19. **Hashemi SM, Ghods S, Kolodgie FD, Parcham-Azad K, Keane M, Hamamdzic D, Young R, Rippy MK, Virmani R, Litt H, Wilensky RL.** 2008. A placebo controlled, dose-ranging, safety study of allogenic mesenchymal stem cells injected by endomyocardial delivery after an acute myocardial infarction. Eur Heart J **29:**251–259.

20. **Ibanez B, Prat-Gonzalez S, Speidl WS, Vilahur G, Pinero A, Cimmino G, Garcia MJ, Fuster V, Sanz J, Badimon JJ.** 2007. Early metoprolol administration before coronary reperfusion results in increased myocardial salvage: analysis of ischemic myocardium at risk using cardiac magnetic resonance. Circulation **115:**2909–2916.

21. **Institute for Laboratory Animal Research (ILAR).** 1996. Guide for the Care and Use of Laboratory Animals. National Academy Press, Washington, D.C.,

22. **Jeremias A, Filardo SD, Whitbourn RJ, Kernoff RS, Yeung AC, Fitzgerald PJ, Yock PG.** 2000. Effects of intravenous and intracoronary adenosine 5'-triphosphate as compared with adenosine on coronary flow and pressure dynamics. Circulation **101:**318–323.

23. **Jeremias A, Whitbourn RJ, Filardo SD, Fitzgerald PJ, Cohen DJ, Tuzcu EM, Anderson WD, Abizaid AA, Mintz GS, Yeung AC, Kern MJ, Yock PG.** 2000. Adequacy of intracoronary versus intravenous adenosine-induced maximal coronary hyperemia for fractional flow reserve measurements. Am Heart J **140:**651–657.

24. **Kennedy JW, Reichenbach DD, Baxley WA, Dodge HT.** 1967. Left ventricular mass. A comparison of angiocardiographic measurements with autopsy weight. Am J Cardiol **19:**221–223.

25. **Kohn F, Sharifi AR, Malovrh S, Simianer H.** 2007. Estimation of genetic parameters for body weight of the Goettingen minipig with random regression models. J Anim Sci **85:**2423–2428.

26. **Kohn F, Sharifi AR, Simianer H.** 2007. Modeling the growth of the Goettingen minipig. J Anim Sci **85:**84–92.

27. **Kondo C, Fukushima K, Kusakabe K.** 2003. Measurement of left ventricular volumes and ejection fraction by quantitative gated SPET, contrast ventriculography and magnetic resonance imaging: a meta-analysis. Eur J Nucl Med Mol Imaging **30:**851–858.

28. **Krause U, Harter C, Seckinger A, Wolf D, Reinhard A, Bea F, Dengler T, Hardt S, Ho A, Katus HA, Kuecherer H, Hansen A.** 2007. Intravenous delivery of autologous mesenchymal stem cells limits infarct size and improves left ventricular function in the infarcted porcine heart. Stem Cells Dev **16:**31–37.

29. **Krombach GA, Kinzel S, Mahnken AH, Gunther RW, Buecker A.** 2005. Minimally invasive close-chest method for creating reperfused or occlusive myocardial infarction in swine. Invest Radiol **40:**14–18.

30. **Lehrke S, Mazhari R, Durand DJ, Zheng M, Bedja D, Zimmet JM, Schuleri KH, Chi AS, Gabrielson KL, Hare JM.** 2006. Aging impairs the beneficial effect of granulocyte colony-stimulating factor and stem cell factor on postmyocardial infarction remodeling. Circ Res **99:**553–560.

31. **Lorenz CH, Walker ES, Morgan VL, Klein SS, Graham TP Jr.** 1999. Normal human right and left ventricular mass, systolic function, and gender differences by cine magnetic resonance imaging. J Cardiovasc Magn Reson **1:**7–21.

32. **Pfeffer MA, Braunwald E.** 1990. Ventricular remodeling after myocardial infarction. Experimental observations and clinical implications. Circulation 81:1161-1172.

33. **Pfeffer MA, Pfeffer JM, Steinberg C, Finn P.** 1985. Survival after an experimental myocardial infarction: beneficial effects of long-term therapy with captopril. Circulation **72:**406–412.

34. **Rosen BD, Lardo AC, Berger RD.** 2006. Imaging of myocardial dyssynchrony in congestive heart failure. Heart Fail Rev **11:**289–303.

35. **Schachinger V, Erbs S, Elsasser A, Haberbosch W, Hambrecht R, Holschermann H, Yu J, Corti R, Mathey DG, Hamm CW, Suselbeck T, Assmus B, Tonn T, Dimmeler S, Zeiher AM.** 2006. Intracoronary bone marrow-derived progenitor cells in acute myocardial infarction. N Engl J Med **355:**1210–1221.

36. **Simonetti OP, Kim RJ, Fieno DS, Hillenbrand HB, Wu E, Bundy JM, Finn JP, Judd RM.** 2001. An improved MR imaging technique for the visualization of myocardial infarction. Radiology **218:**215–223.

37. **Slavin GS, Saranathan M.** 2002. FIESTA-ET: high-resolution cardiac imaging using echo-planar steady-state free precession. Magn Reson Med **48:**934–941.

38. **Smith AC, Swindle MM.** 2006. Preparation of swine for the laboratory. ILAR J **47:**358–363.

39. **van Gilst WH, Kingma JH, Peels KH, Dambrink JH, St John SM.** 1996. Which patient benefits from early angiotensin-converting enzyme inhibition after myocardial infarction? Results of one-year serial echocardiographic follow-up from the Captopril and Thrombolysis Study (CATS). J Am Coll Cardiol **28:**114–121.

40. **Wakeman DR, Crain AM, Snyder EY.** 2006. Large animal models are critical for rationally advancing regenerative therapies. Regen Med **1:**405–413.

41. **Wynne J, Green LH, Mann T, Levin D, Grossman W.** 1978. Estimation of left ventricular volumes in man from biplane cineangiograms filmed in oblique projections. Am J Cardiol **41:**726–732.